Observation and study of centrally produced pion clusters in 28.5-GeV/c p-p interactions*

A. R. Erwin, E. H. Harvey, and G. P. Larson
Department of Physics, University of Wisconsin, Madison, Wisconsin 53706

G. B. Collins, J. R. Ficenec, B. C. Stringfellow,† and W. P. Trower
Department of Physics, Virginia Polytechnic Institute and State University, Blacksburg, Virginia 24060

L. J. Gutay, A. Laasanen, and R. B. Willmann
Department of Physics, Purdue University, Lafayette, Indiana 47907

E. W. Anderson,‡ G. P. Fisher,§ E. Lazuras,‖ L. von Lindern,¶ A. Ramanauskas,** P. Schubelin,† A. M. Thorndike and F. Turkot††
Brookhaven National Laboratory, Upton, New York 11973
(Received 5 April 1976)

A double-arm spectrometer is used to identify a pion cluster produced in central p-p collisions at 28.5 GeV/c. Cluster properties studied are angular momentum, quantum statistics, multiplicity, and effective mass. There is some speculation on the production mechanism.

INTRODUCTION

The work presented here began as an attempt to find angular momentum in the cloud of pions produced in 28.5-GeV/c p-p collisions.[1,2] Angular momentum was indeed found, but it could be removed with surprising ease by a reasonable, systematic cut that eliminated peripheral, low-mass clusters from the data sample. The remaining pions formed a remarkable Bose gas which had never before been so cleanly isolated. The major portion of this work is now devoted to the study of this gas and its unique origin insofar as our experimental apparatus permits.[3]

EXPERIMENTAL ARRANGEMENT AND PROCEDURE

The apparatus used is shown in Fig. 1 and is described in more detail elsewhere.[4] It was employed as a double-arm spectrometer for protons in this experiment. A Čerenkov counter in the high-momentum spectrometer (HMS) and a Čerenkov counter augmented by a time-of-flight measurement in the low-momentum spectrometer (LMS) produced a double-arm trigger on two outgoing protons. Use of wire spark-chamber planes in these two arms gave precise momentum and angle measurements for the two protons. The resolutions were $\Delta p/p \approx \pm 0.3\%$ at 20 GeV/c, $\Delta\theta \approx \pm 0.2$ mrad for the HMS and $\Delta p/p \approx \pm 1.0\%$ at 2.0 GeV/c, $\Delta\theta \approx \pm 1.0$ mrad for the LMS. From time-of-flight measurements below 1 GeV/c in the LMS we estimate K contamination in the trigger to be less than 5%.

The run procedure consisted of placing the HMS in one of four positions, referred to as positions 1.0, 2.0, 2.5, and 3.0, and then cycling the LMS through eight positions, 4.0–11.0. Positions were such as to preclude elastic p-p events and all events with very small momentum transfer to a proton. A crude estimate indicates that these double-arm p-p events are representative of a sample not exceeding 5% of all p-p interactions.

Large momentum transfer to the protons was rather thoroughly investigated, but only for cases where the two protons were coplanar to within several degrees. It is difficult to find a satisfactory graphic display of the phase space covered by this experiment, but Fig. 2 gives some measure of what was accomplished in terms of the four-momentum transfer, t_1, to the HMS proton and the missing mass s_2 of the system recoiling from the HMS. The contours show the area of the figure that was actually populated by data for each HMS arm position. The theoretical acceptance of the apparatus was always considerably larger than these contours, but in any given run the dynamics of the collisions strongly favored the low-t regions of the acceptance. Low event rates and finite running time prevented running at positions which would have yielded higher-momentum-transfer events. A figure with very similar characteristics exists for the LMS but is not shown.

The nontrigger particles were detected and measured in the vertex spectrometer, a set of nine cylindrical, magnetostrictive spark chambers in a 10-kG field. Potential experimental biases in such a system are numerous and have been studied by us in much detail. Fortunately these biases are either negligible or irrelevant for the topic of this paper. Perhaps two are worthy of mention here.

The cylindrical spark chambers cannot detect

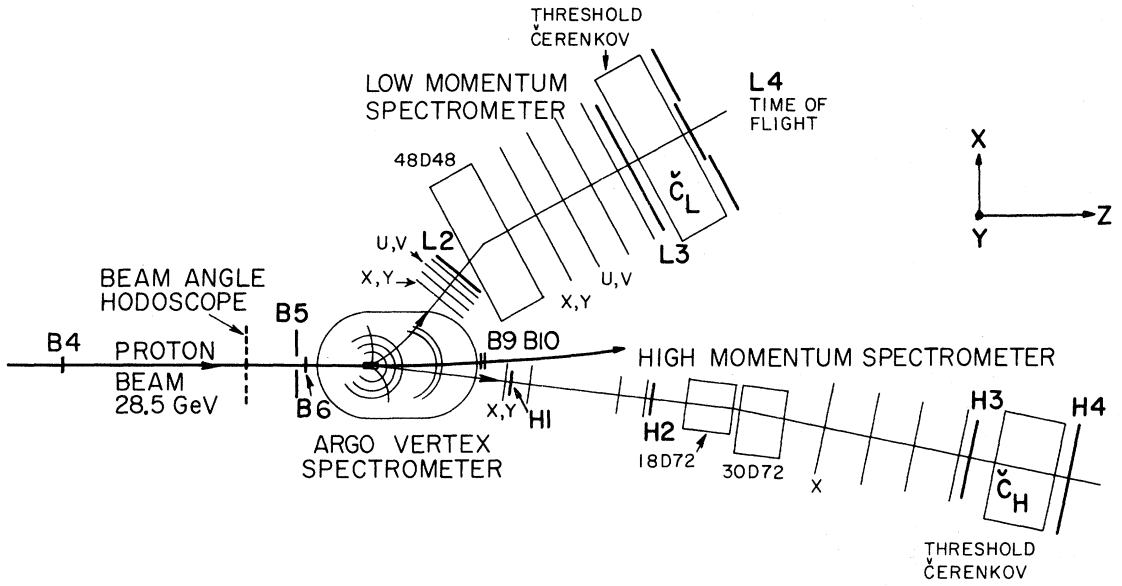

FIG. 1. Multiparticle Argo spectrometer system schematic diagram.

particles with dip angles so large that they escape along the cylinder axis. In practice we require three chambers to fire in order to identify a track. The geometry of the third chamber with respect to the target is such that for dip angles whose magnitude exceeds 40°–50° we should begin to experience appreciable losses. Figure 3 is a plot of pion dip angles in the vertex spectrometer for all double-arm triggered events. Because of the forward collimation of secondaries in the laboratory system, we can estimate from the figure a track loss of only several percent due to this effect.

A more significant loss that must be kept in mind in later analysis of the data is that caused by the magnetic field, which prevents pions with momentum less than 80–100 MeV/c from reaching the third spark chamber from the target. Pions with less than 100 MeV/c in the laboratory all transform into the backward hemisphere of the center-of-mass system and have momentum vectors that lie within ±10° of the beam axis with magnitudes that range from 250 MeV/c to 1.0 GeV/c.

This loss is most dramatically illustrated in

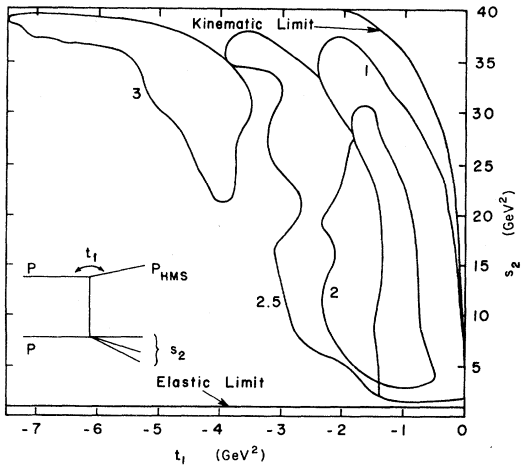

FIG. 2. Observed data as a function of the mass s_2 recoiling from the proton in the high-momentum arm with a momentum transfer t_1.

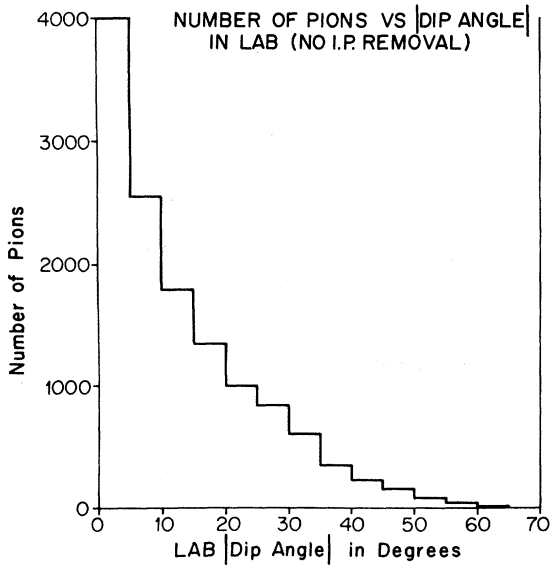

FIG. 3. Experimental distribution of dip angles with respect to the plane of the floor for pions in the vertex spectrometer. (I.P. stands for isobaric pion.)

Fig. 4, where the angular distribution of all pions in the center of mass is shown with respect to the x axis, which is perpendicular to the beam and lies in the plane of the experimental floor as defined in Fig. 1. As expected, the loss occurs only in the backward hemisphere and only within 10° of the beam axis. Assuming a $\sin^2\theta$ distribution for tracks in this plot, we estimate a loss of about 11% for the tracks in the backward hemisphere due to this effect.

ANGULAR MOMENTUM SEARCH

There have frequently been proposals to study the aggregate angular momentum of the final-state pions found in high-multiplicity events.[5-7] Most of these schemes involve defining a coordinate system on an event-by-event basis which will highlight any asymmetry that might exist. Results are necessarily difficult to interpret because of the nature of the coordinate system.

The motivation for such an angular momentum search is nevertheless very strong because of the potential insight it may give into the pion production mechanism. Two extreme examples may suffice here. In a geometrical model such as that of Yang and Wu[8] one might anticipate "pionization" as depicted in Fig. 5(a). High momentum and finite impact parameters would certainly suggest angular momentum in the cloud of produced pions. On the other hand, if the pions are produced by the collision of pointlike constituents or partons[9] in hadrons as in Fig. 5(b), then the zero impact

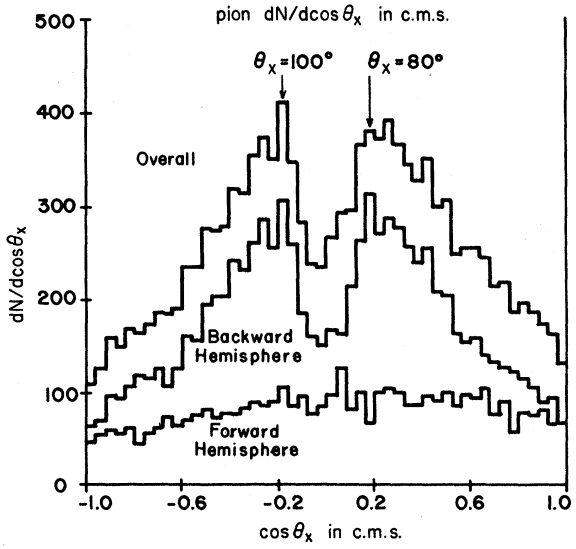

FIG. 4. Center-of-mass angular distribution of pions with respect to the x axis showing losses of pions with lab momenta below 100 MeV/c. (c.m.s. stands for center-of-mass system.)

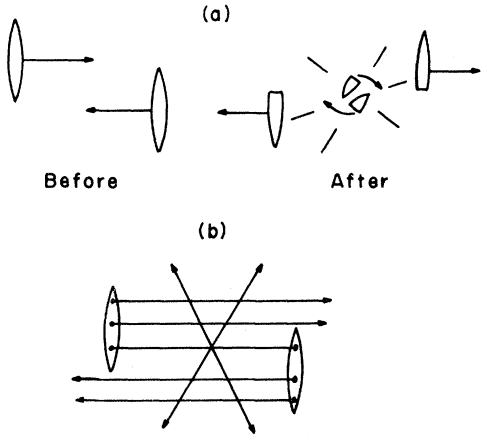

FIG. 5. (a) Intuitive picture for origin of angular momentum of a pion cloud in a fragmentation description. (b) Schematic of a pointlike parton collision giving no angular momentum to the pion cloud.

parameter would suggest no angular momentum in the resulting cloud of pions.

The most obvious quantization axis for a spin analysis of this pion cloud is the normal to the plane of the two outgoing protons. To a good approximation this axis is also the normal to the experimental floor. Using the precise momentum measurements of the two protons one can transform to the rest system of the pion cloud and plot the distribution of the cosine of the charged-pion momentum vectors with respect to the floor normal.

The upper curve of Fig. 6 is a plot of this cosine, $\cos\theta_y$. For angular momentum aligned along the normal one expects a distribution modulated by the $\sin^2\theta$ characteristic of the square of the associated Legendre polynomials, $P_l^m(\cos\theta)$. This would appear as a preferential production of pions in the plane of the floor. Such a preference does appear in Fig. 6, indicating that rather high partial waves are contained in the pion cloud as we have defined it.

As was pointed out earlier, the axis of symmetry for the cylindrical spark chambers is also normal to the floor and should result in a loss of pions with a dip that exceeds 40°–50° with respect to the floor. The experimental distribution of pions (Fig. 3) in the laboratory is such that this loss can in no way account for the bump at $\cos\theta_y = 0$ in Fig. 6 and is small enough that no correction for it has been made in the discussion that follows.

ISOBARIC-PION CUTS

A close study of the pion momentum distributions (not shown) in the cloud frame of reference reveals that an excess of pions prefers to travel in

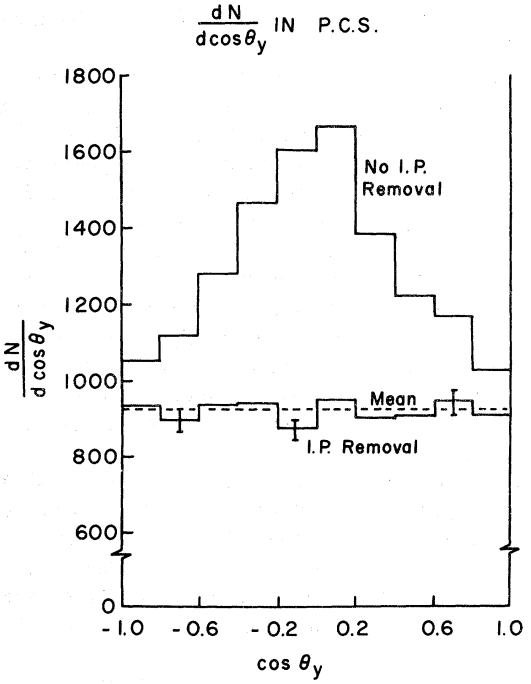

FIG. 6. Upper histogram: the angular distribution of pions with respect to the floor normal in the rest system recoiling from the two trigger protons. Lower histogram: the same distribution with isobar-associated pions removed. (P.C.S. stands for pion-cloud system.)

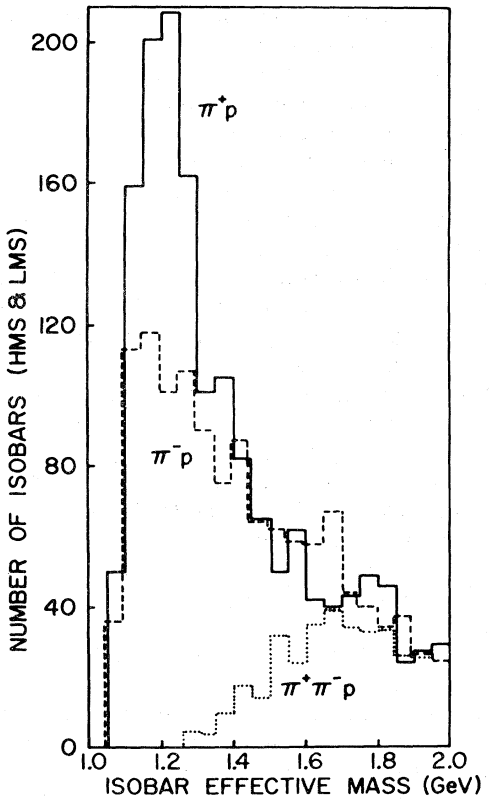

FIG. 7. Observed mass spectra of baryon isobars.

the proton direction, especially if the proton is peripherally produced. These pions would seem most likely to originate from isobar decay. If an isobar is produced and decays in the plane of the floor, its decay proton can trigger our system. Including its decay pion in the cloud could then be expected to introduce angular momentum normal to the floor or an excess of pions in the plane of floor for the trigger events.

If there is a pionization cloud, then one should include neither the protons nor the isobar fragments in the angular momentum analysis of the cloud. Realizing that pions from isobar decay cannot be excluded in a unique way, we will nevertheless attempt in the remainder of this paper to analyze the data in such a way as to minimize the number of isobaric pions (I.P.'s) in the data sample.

Our first attempt to remove isobaric pions from the data is based on three characteristics which seem to typify pp isobar production at 30 GeV/c (see Ref. 10):

1. The isobar has mass less than 2.0 GeV/c^2.
2. The momentum transfer to the isobar is less than $|t|=1.0$ GeV^2.
3. Allowed observable charged isobar states are $p\pi^+$, $p\pi^-$, $p\pi^+\pi^-$.

The procedure is to associate all possible $\pi^\pm$ and $\pi^+\pi^-$ pairs with each final-state proton, selecting those states as isobar candidates which pass requirements 1 and 2. If more than one isobar candidate involving the same proton is possible, that exhibiting the smallest momentum transfer is selected.

These selection criteria result in assigning at least one isobar to ~60% of our events. Roughly 30% of all charged pions are identified as isobaric pions from isobar decay. Most isobars involve only a single pion, and only ~10% of the events have two isobars.

Mass spectra from the HMS- and LMS-selected isobars are shown in Fig. 7. The π^+p spectrum peaks near the $\Delta(1238)$, but the π^-p and $\pi^+\pi^-p$ spectra do not show the strong influence of known isobars. It is interesting to note that the π^-p mass peaks at a value which is even slightly lower than the π^+p peak. The failure to see distinct isobars in these spectra is not a matter of experimental resolution, since we can easily identify such peaks when the apparatus is used as a single-arm spectrometer. Perhaps we should call these low-mass associations clusters, but we will continue to refer to them as isobars because the characteristics of isobar production provided the motivation for

the cuts. We expect that the general shape of both the isobar mass spectrum and decay spectrum will be influenced by the laboratory-system acceptance of the spectrometer arms. Since a study of the acceptance requires a detailed model of isobar production and decay, we have been unable to make quantitative corrections to these spectra.

The momentum-transfer spectrum of the selected isobars has a slope of 1.0–1.5 GeV^{-2} rather than the typical nondiffractive exponential slope of 3–5 GeV^{-2} found for two-body final states at this energy. Again, this spectrum is probably influenced by the acceptance of the spectrometer arms.

When as isobar (N^*) has been identified according to the above prescription, a new rest frame for the pion cloud can be defined using the momentum vectors of the baryons, protons, or N^*'s as the case may be. The normal to the floor is replaced as a quantization axis by the cross product of the outgoing-baryon momentum vectors, $\vec{p}_p \times \vec{p}_p$, $\vec{p}_{N^*} \times \vec{p}_p$, or $\vec{p}_{N^*} \times \vec{p}_{N^*}$. In practice this axis remains essentially normal to the floor. Excluding isobaric pions, the new distribution of the pion cosines with respect to the normal in the cloud rest frame is shown in the lower histogram of Fig. 6. All evidence for angular momentum disappears when the isobaric pions are removed.

The sensitivity of this result and those that follow to the exact specifications of the isobar cut can be displayed by plotting the change in the pion-cloud angular distributions as these specifications are changed. We parameterize the isotropy of a $\cos\theta$ distribution by an inside-to-outside ratio, I/O, where I is the number of tracks with $-0.5 < \cos\theta < +0.5$, and O is the number with $|\cos\theta| > 0.5$. An isotropic distribution will have $I/O = 1.0$.

The I/O ratios along three orthogonal axes in the pion-cloud system are plotted in Fig. 8 as a function of the isobaric mass cut for three different cuts on momentum transfer. It appears that the cuts we have chosen are sufficient to produce near isotropy in the pion cloud system without excessive pion removal. More detailed study indicates that a larger-t cut could be used for data collected at the large-angle settings of the spectrometer arms, since apparently some leading baryon clusters with higher momentum transfer are produced there. The number of these events in our data is small and no special cut has been made for them.

Some fraction of the isobars will decay with a neutral pion. Since this pion is not detected, it will not mistakenly appear in any pion cloud distribution. We have studied two secondary consequences of missing isobaric π^0's, however, and find that they are not important in the present studies.

If an isobaric π^0 is not detected, transformation to the cloud system is made using the momentum of the proton alone rather than that of the proper isobar. This was studied by ignoring charged isobaric pions in our sample and transforming to the cloud system using only the remaining proton momentum. The shape of pion-cloud momentum distributions remained unchanged by this except for one bin in the distribution of components along the proton direction which was depleted about 6%.

If the proper isobaric pion is neutral, one might instead select incorrectly a charged pion as the

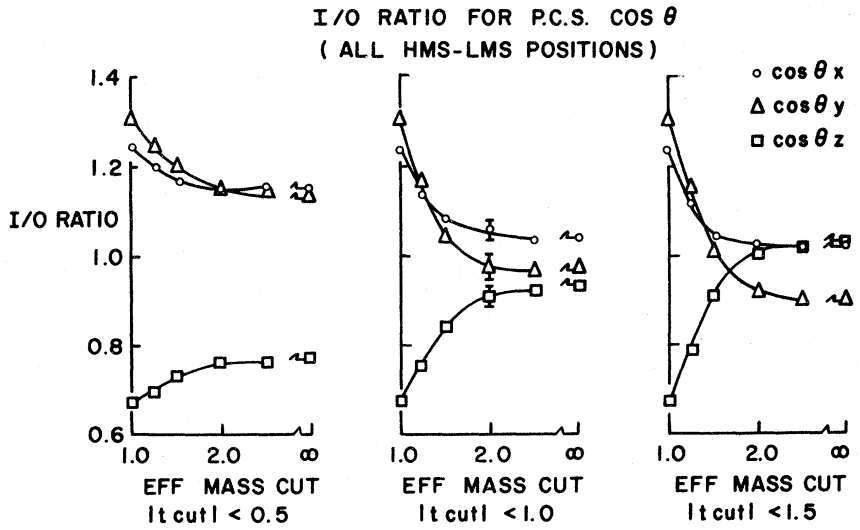

FIG. 8. Ratio of I ($|\cos\theta| < 0.5$) to O ($|\cos\theta| > 0.5$) events for distributions along three orthogonal axes in the pion-cloud rest system as a function of isobar mass and t cuts.

isobaric pion. This situation was simulated as above using known isobar events, ignoring the charged isobaric pion, and selecting a secondary isobaric pion when possible. Again the only momentum distribution affected was the one for components along the direction of the recoil proton. This distribution suffered a depletion of about 30% at small angles with respect to the proton owing to incorrect removal of cloud pions as isobaric pions. The real effect due to unobserved π^0's must be even smaller since only 16% of events with a charged isobaric pion had a second pion that could satisfy the cuts required in t and M^* for isobars.

APPLICATION TO A QUARK MODEL

If one assumes that the pion cloud was produced by the collision of two quarks, then the isotropy of the cloud has some significance in placing a limit on the quark radius. This can be done if the cloud isotropy implies zero angular momentum or s-wave production. In general, this is a safe assumption, since otherwise a special conspiracy of partial waves (such as that provided by no alignment of angular momentum) is required to produce isotropy.

If protons are composed of three quarks, then each quark in the c.m. system will on the average have one third of the beam momentum, 1.2 GeV/c in our case. The impact parameter for the collision must be less than or equal to an s-wave radius for this quark momentum, $\lambda\!\!\!^{-} = 0.16\times10^{-13}$ cm. Thus we might conclude that the quark interaction radius is this small or smaller.

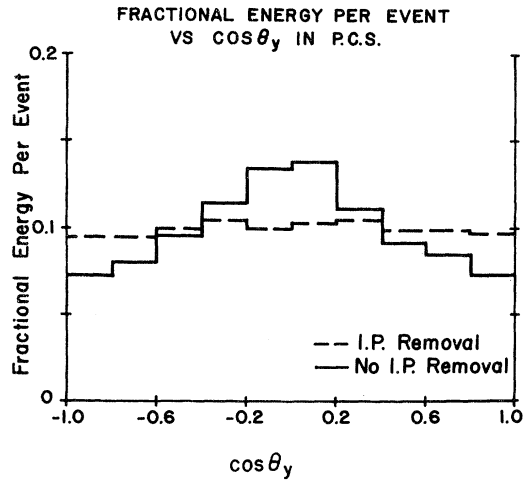

FIG. 9. Fraction of energy per event emitted as a function of angle with respect to floor normal in the cloud system. Solid histogram is for all pions. Dashed histogram has isobaric pions removed.

ENERGY DISTRIBUTION IN PION CLOUD

In contrast to two-body final states, multiparticle final states have the possibility that the angular distribution of the particle directions need not be the same as the angular distribution of energy flux. To study this we observe the fraction of the energy radiating in a specific direction on an event-by-event basis. Figure 9 shows this angular distribution of energy with respect to the floor normal in the pion-cloud rest system. Of the three orthogonal distributions this was the most anisotropic before removal of the isobaric pions.

MOMENTUM DISTRIBUTION IN THE PION CLOUD

The isotropy of the pion cloud in the angular distributions for particle and energy flux is consistent with a statistical gas model in a reference frame with no preferred direction. We have tried fitting the momentum distribution in the pion cloud to

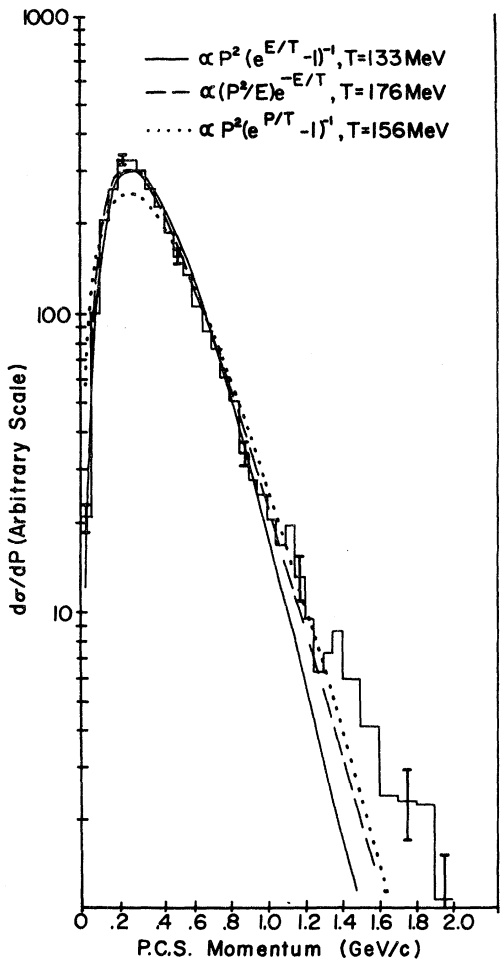

FIG. 10. Momentum distribution of pions in the pion-cloud system with three statistical fits to the data.

permutations of several statistical distributions which appear in the literature. Two of the better fits are shown as the solid and dashed curves in Fig. 10. Exponentials in the momentum such as the dotted curve, which are sometimes used,[11] are unsatisfactory, especially in the region where momentum is comparable to the pion mass.

All models fail to give an adequate fit at the highest momentum. Since the amount of data in this region has dropped two orders of magnitude, the spectrum at high momentum could be greatly influenced by the prescription for removing isobaric pions. In fact, the percentage of isobaric pions removed from the distributions rises from ~25% near $p=0$ to ~55% above $p=1.5$ GeV/c.

A better distribution for comparison with statistical models is the component of momentum along the floor normal, p_y. This is because the percentage of isobaric pions removed from the p_y data sample decreases rapidly with increasing p_y to about 10% above $p_y=0.5$ GeV/c. An excellent fit (χ^2 probability = 78%) to this spectrum using a Bose-Einstein gas with a simple momentum phase space, p^2dp, is shown in Fig. 11. However, use of an invariant phase-space factor, p^2dp/E, gives rather poor results (χ^2 probability = 2%). The gas temperature obtained in the best fit, $T=132$ MeV, is comparable to that commonly obtained in fits to transverse-momentum spectra.

MULTIPLICITY AND MASS

The relative cross section for producing pion clouds with different charged multiplicities is shown in Fig. 12. Errors indicated are statistical only. Relative cross sections in this figure were obtained by weighting each data point by the inverse of the beam flux used in a particular run. Systematic errors may be comparable to the statistical ones, but they have not been included because of

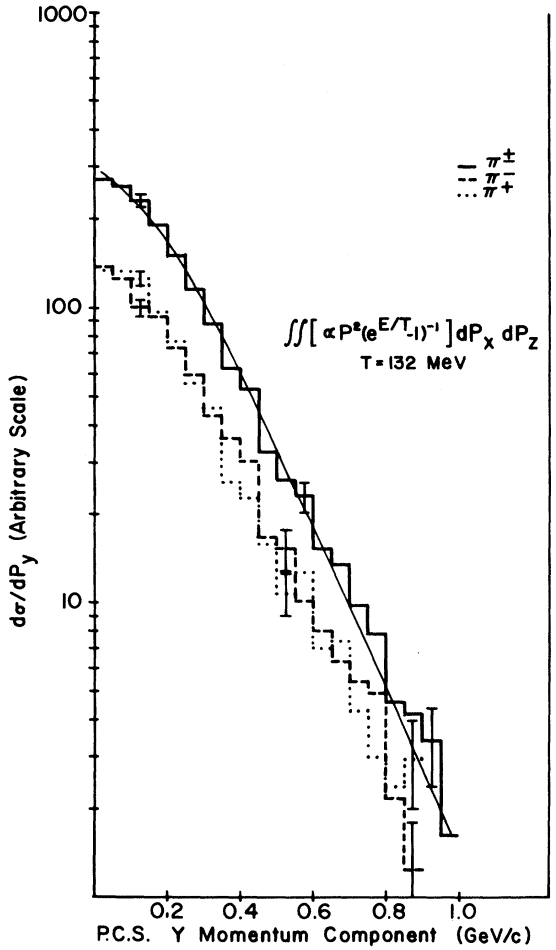

FIG. 11. Distribution of pion momentum components along the floor normal in the cloud system. Smooth curve is a fit to Bose-Einstein statistics.

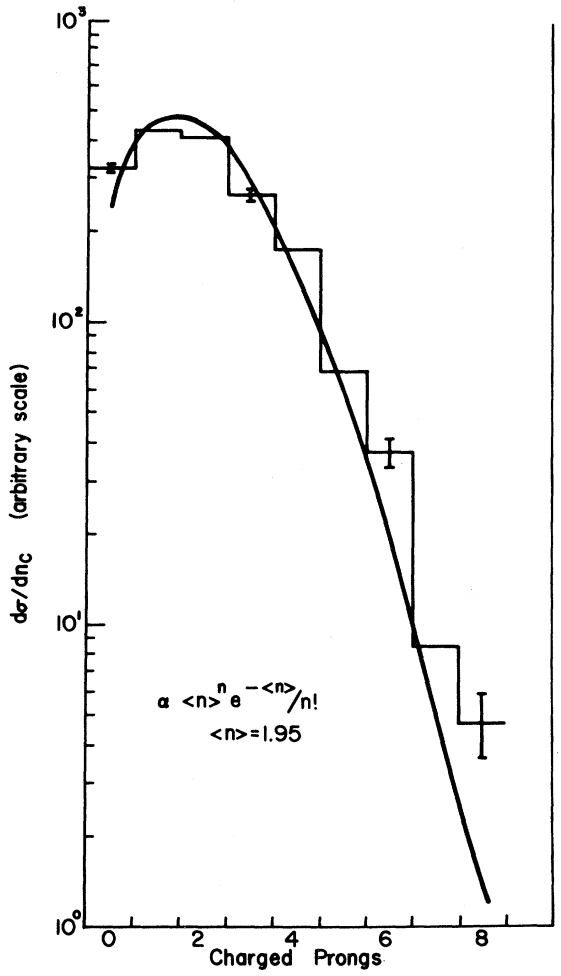

FIG. 12. Multiplicity distribution of charged prongs in the pion cloud.

the difficulty of evaluating them for our double-arm triggers.

In spite of the crudeness of the cross-section calculation, the multiplicity appears to exhibit the character of a Poisson distribution. This further strengthens the notion that the pions are produced in a random, statistical manner.

Figures 13 and 14 give the distribution of cloud mass, obtained from the recoil momenta of the protons and/or isobars, for each value of charged multiplicity. With the possible exception of the $n_c = 0$ case these distributions tend to converge to the same magnitude for a cloud mass $M_c \gtrsim 4$ GeV/c^2 when statistics are reasonably good ($n_c \leq 6$).

The relation between the average charged multiplicity and the total pion-cloud mass is drawn with the solid-line histogram in Fig. 15 and is seen to be linear up to masses of 5.0 GeV/c^2 and multiplicities of $\langle n_c \rangle \approx 4$. Linear relations such as this have been observed in the same mass range for pions from e^+e^- annihilation,[12] for hadron clusters recoiling against a peripheral proton in pp collisions,[13] and for hadron clusters recoiling against a peripheral proton or pion in πp collisions.[14] The slopes and intercepts in some cases differ from ours, but this is most likely due to the manner in which these experiments defined the cluster, computed the mass, or accounted for neutral pions.

The dashed curve of Fig. 15 shows the effect of ignoring the role of the neutral particles when studying correlations between mass and multiplicity. When the average charge multiplicity is plotted as a function of the effective mass of the charged particles, the relation is no longer linear.

Figure 16 probably makes the mechanism of this easier to understand. In the framework of a statistical model where each pion contributes the same average energy to the effective mass, the charged mass should be $\frac{2}{3}$ the total mass recoiling from the leading baryons. However, if the number

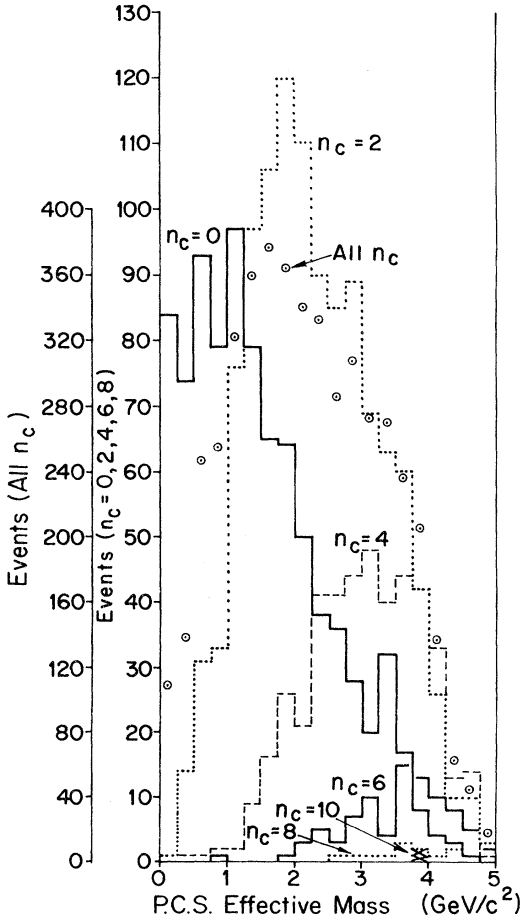

FIG. 13. Distribution of pion-cloud mass recoiling from the leading baryons for even numbers of charged pions in the cloud.

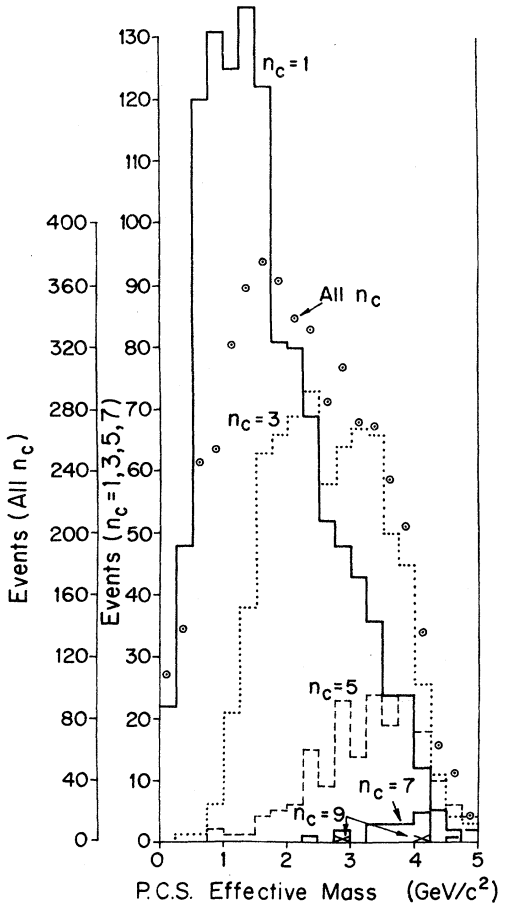

FIG. 14. Distribution of pion-cloud mass recoiling from the leading baryons for odd numbers of charged pions in the cloud.

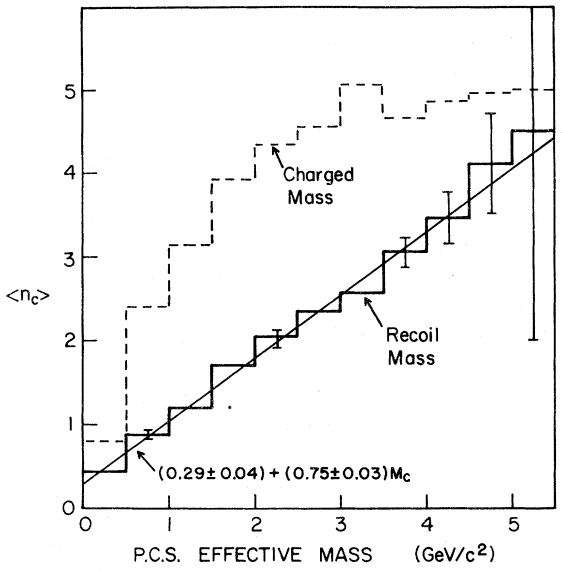

FIG. 15. Average number of charged pions as a function of cloud mass. Solid histogram has cloud mass computed by recoil from baryons. Dashed histogram uses the effective mass of the charged pions as the cloud mass.

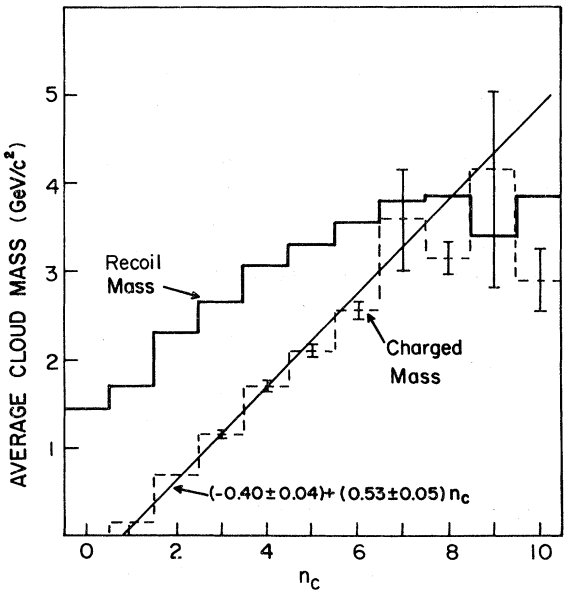

FIG. 16. Average cloud mass as a function of the charged-pion multiplicity of the cloud. Solid histogram uses the cloud mass computed from baryon recoil. Dashed histogram uses the effective mass of the charged pions.

of charged particles is the very highest allowed by phase space, all particles must be charged, and the recoil mass will equal the charged mass. At the other extreme, when the number of charged particles is much less than the average number expected, a larger proportion of the mass will be neutral.

For masses above 4.5 GeV/c^2 data on peripheral clusters suggest[13] $\langle n_c \rangle \propto \ln M_c$, but the cluster is probably not so well defined as the pion cloud in this experiment. The linear relation observed is expected if one is dealing with a statistical model for nuclear matter of the Hagedorn type.[15] On the other hand, multiperipheral models suggest the $\ln M_c$ behavior,[16] which can in no way fit our data at small M_c.

The absence of a zero intercept at $M_c = 0$ in Fig. 15 is quite proper since the smallest cloud mass we deal with is that of a single pion. Furthermore, at that mass $\langle n_c \rangle = 0.40 \pm 0.04$, which is consistent with about 50% of single-pion clouds being charged rather than 67%, which one might expect if all charges were equally preferred by the cloud production process.

MESON RESONANCES IN THE CLOUD

In the mass distributions of Figs. 13 and 14 one can see little evidence of recognized pion resonances. This is certainly consistent with what we have seen so far with respect to a Bose gas, but it is hard to imagine pions confined in a small phase-space volume that will not rescatter and emerge ultimately with some evidence of a strong resonance like the ρ meson.

Since combinatorial background may obscure evidence for a ρ meson, we have plotted the mass distribution for all $\pi^+\pi^-$ pairs in the pion cloud in Fig. 17. For completeness we have also plotted the same spectrum for all pions without isobaric-pion removal from the pion system. A Brookhaven group has recently reported equal amounts[17] of ρ and π^- production in $\pi^+ p$ interactions at 22 GeV for transverse momentum above 1.0 GeV/c. Because the cloud has no distinguishable transverse direction we have made cuts on the data for the resultant momentum, p_M, of the $\pi^+\pi^-$ pair. The only possible evidence for ρ production appears in Fig. 17(c) for pair momenta above 1.0 GeV/c and amounts at most to ~8% of the π^- production. However, since our triggered data only represent about 2% of an unbiased bubble-chamber run, we may not necessarily see the same phenomena.

Our ability to detect a ρ resonance depends on the mass resolution of the vertex spectrometer, which is not as precise as that of the two proton arms which are used to determine the overall cloud mass. A typical ρ event with $p_\rho = 1.0$ GeV/c has a mass resolution better than 10 MeV/c^2 for nine-chamber detection of both tracks. Even for a 2-GeV/c ρ detected by six chambers at high p_T,

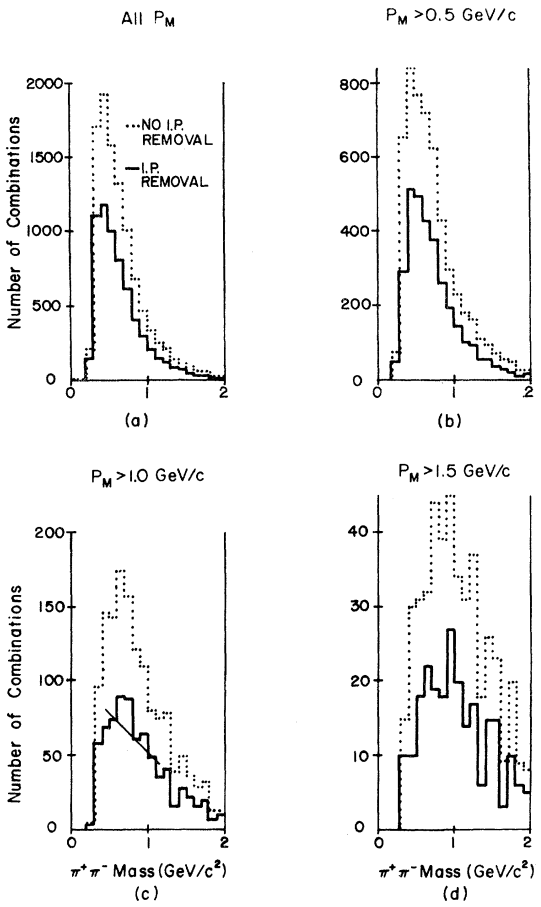

FIG. 17. Mass distribution of $\pi^+\pi^-$ pairs in the cloud for different cuts on the momentum, P_M, of the pair in the cloud system. Dashed histogram includes isobaric pions.

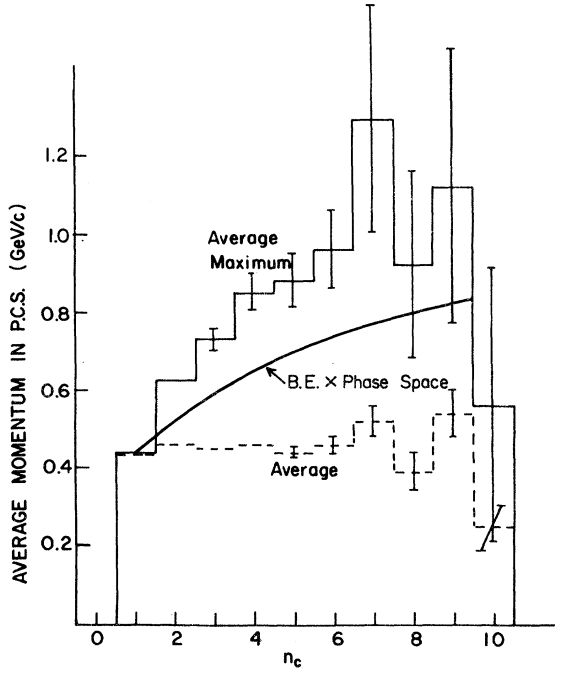

FIG. 18. Dashed histogram: the average pion momentum in the cloud vs charged prongs. Solid histogram: the average of the maximum momentum in each event vs charged prongs. The curve is the average maximum momentum expected from a model with Bose-Einstein (B.E.) statistics.

a mass resolution of 50–60 MeV/c^2 seems representative, and one would still expect to see a ρ with a width of 150 MeV/c^2.

PRODUCTION MECHANISMS

The usual variables which one might use to study the production process are not readily available in this experiment. Since all the running was at one energy we have no s dependence, and the t dependence is somewhat obscured by the complex acceptance of the double-arm trigger and associated magnetic fields. However, it is certain that the interaction is not highly peripheral, since the t dependence at either baryon vertex is between e^t and $e^{1.5t}$

The π^+p and π^-p mass spectra of the selected isobars in Fig. 7 are not inconsistent with general $1/M^2$ behavior when a correction is considered for the mass dependence of the trigger. In fact, subtraction of a fitted $1/M^2$ background from the $p\pi^+$ mass spectrum yields a substantial amount of 1238 isobar production with the correct width. A similar fit works well for the $p\pi^-$ spectrum but does not yield any convincing evidence for accepted resonances.

A $1/M^2$ variation in the cross section is typical experimentally of diffractively produced clusters[18] and would be expected for triple-Pomeron coupling.[16] However, the t dependence of our cross section does not seem to be consistent with any type of Pomeron exchange.

The magnitude of the cross section we observe for central-cluster production does not single it out as an especially rare process, although it may be relatively small since it has not been a prominent feature in bubble chamber experiments. Scaling up our data in the plane of the floor for unobserved azimuthal angles, we estimate a cross section of ~1 mb. This includes no allowance for cluster production in which the protons are not approximately coplanar and no correction for trigger losses at large isobar masses. With these possibilities properly accounted for one might find the cross section for central-cluster production to be as large as several millibarns.

If the cluster production results from parton collisions, one expects the partons to give two jets

in the cloud frame.[19] A flat rapidity distribution along a jet axis implies that the most energetic pion will have on the average about $\frac{1}{2}$ of the initial parton (jet) momentum of 1.2 GeV/c. Figure 18 shows the average value of the maximum momentum p_{max} in the cloud system of each event plotted as a function of the charged multiplicity of the cloud. Also plotted is the average momentum in the cloud system of each event. $\langle p_{max} \rangle$ is somewhat greater than the average momentum for higher multiplicities. The lower value for charged multiplicity $n_c = 1$ or 2 might be expected if these clouds have a larger than average admixture of neutral pions, making it less likely that p_{max} is observed.

The curve in Fig. 18 is the expected value of $\langle p_{max} \rangle$ if the maximum charged momentum in a cloud is selected from a computer-generated Bose-Einstein distribution with n_c particles and a mean momentum which agrees with experiment. This curve, although lower, shows the same general increase with n_c as the data. Since it does not accurately account for the role of neutral pions, and since the statistical accuracy of the data becomes poor for large n_c, it is not possible here to draw any conclusion about the emergence of a jet structure at this energy.

CONCLUSIONS

We have observed a class of events in p-p collisions which exhibits a cluster of pions that can be easily separated from the leading clusters that have baryon number. The energy and angular distributions of pions in the cluster are isotropic. Bose-Einstein statistics with a temperature $T = 132$ MeV are needed to describe the momentum distribution of the pions. A linear relation between cluster mass and charged multiplicity is consistent with a statistical model. The Poisson distribution of multiplicity in the pion cluster is also consistent with such a statistical picture. Essentially no evidence was found for meson resonances in the pion cloud.

The lack of evidence for angular momentum in the pion cluster suggests a basic collision radius of ~0.1 Fermi or less for the production process. This is not inconsistent with the relatively broad momentum-transfer spectrum to the leading baryon clusters.

A cross section of about 1 mb for events with our coplanar baryon trigger topology indicates that this type of pion cluster formation is a relatively important part of p-p interactions at 28.5 GeV/c.

---

*Work performed under the auspices of the Energy Research and Development Administration, contracts numbers E(11-1)-881, E(30-1)-16, and AT(11-1)-1428.

†Present address: Centre de Recherches Nucleaires, Labo PNPP-HE, Boite Postale 20/CRO, 67037 Strasbourg CEDX, France.

‡Present address: Iowa State University, Ames, Iowa 50010.

§Present address: R&D Associates, P. O. Box 3580, Santa Monica, California 90401.

||Present address: Singer-Kearfott Co., 150 Totowa Road, Wayne, New Jersey 07470.

¶Present address: Max-Planck-Institut für Psychiatrie, 8 München 23, Kraepelinstrasse 2, West Germany.

**Deceased.

††Present address: Fermi National Accelerator Laboratory, P. O. Box 500, Batavia, Illinois 60510.

[1]A. R. Erwin *et al.*, in *Proceedings of the IVth International Symposium on Multiparticle Hadrodynamics, Pavia, Italy, 1973*, edited by F. Duimio, A. Giovannini, and S. Ratti (INFN, Pavia, 1973), p. 293.

[2]A. Ramanauskas *et al.*, in *Proceedings of the Vth International Symposium on Multiparticle Hadrodynamics, Eisenach and Leipzig, 1974*, edited by G. Ranft and J. Ranft (Karl-Marx-Universität, Leipzig, 1974), p.401.

[3]G. P. Larson, Ph.D. thesis, University of Wisconsin, Madison, 1975 (unpublished).

[4]E. W. Anderson *et al.*, Nucl. Instrum. Methods 122, 587 (1974).

[5]We would like to thank R. G. Glasser and J. Lamsa for informing us of their unpublished work in this area. For application of this approach see R. G. Glasser *et al.*, Phys. Lett. 53B, 387 (1974).

[6]R. Raczka and A. Raczka, in *Proceedings of the XII International Conference on High Energy Physics, Dubna, 1964*, edited by Ya. A. Smorodinskii (Atomizdat, Moscow, 1966).

[7]P. Kostka, H. Nowak, H. Schiller, and J. Gajewski, Nucl. Phys. B86, 1 (1975).

[8]T. T. Wu and C. N. Yang, Phys. Rev. 137, B708 (1965).

[9]R. P. Feynman, Phys. Rev. Lett. 23, 1415 (1969).

[10]E. W. Anderson *et al.*, Phys. Rev. Lett. 19, 198 (1967).

[11]W. H. Sims *et al.*, Nucl. Phys. B41, 317 (1972).

[12]C. Morehouse, private communication.

[13]J. Whitmore, Phys. Rep. 10C, 273 (1974).

[14]R. N. Diamond *et al.*, Nucl. Phys. B62, 128 (1973).

[15]R. Hagedorn, Nuovo Cimento 56A, 1027 (1968).

[16]W. R. Frazer *et al.*, Rev. Mod. Phys. 44, 284 (1972).

[17]H. A. Gordon, M. M. Habibi, K.-W. Lai, and I. Stumer, Phys. Rev. Lett. 34, 284 (1975).

[18]F. C. Winkelmann *et al.*, Phys. Rev. Lett. 32, 121 (1974).

[19]J. D. Bjorken, Acta Phys. Polon. B5, 893 (1974).